



HAL
open science

Cellulose nanocrystals modification by grafting from ring opening polymerization of a cyclic carbonate

Michaël Lalanne-Tisné, Samuel Eyley, Julien de Winter, Audrey Huret, Wim Thielemans, Philippe Zinck

► To cite this version:

Michaël Lalanne-Tisné, Samuel Eyley, Julien de Winter, Audrey Huret, Wim Thielemans, et al.. Cellulose nanocrystals modification by grafting from ring opening polymerization of a cyclic carbonate. Carbohydrate Polymers, 2022, Carbohydrate Polymers, 295, pp.119840. 10.1016/j.carbpol.2022.119840 . hal-03759014

HAL Id: hal-03759014

<https://hal.univ-lille.fr/hal-03759014>

Submitted on 21 Nov 2023

HAL is a multi-disciplinary open access archive for the deposit and dissemination of scientific research documents, whether they are published or not. The documents may come from teaching and research institutions in France or abroad, or from public or private research centers.

L'archive ouverte pluridisciplinaire **HAL**, est destinée au dépôt et à la diffusion de documents scientifiques de niveau recherche, publiés ou non, émanant des établissements d'enseignement et de recherche français ou étrangers, des laboratoires publics ou privés.



Distributed under a Creative Commons Attribution - NonCommercial - NoDerivatives 4.0 International License

1 **Cellulose nanocrystals modification by grafting from ring opening**
2 **polymerization of a cyclic carbonate**

3 Michael Lalanne-Tisné^{1,2}, Samuel Eyley¹, Julien De Winter³, Audrey Favrelle-Huret², Wim Thielemans^{1*},
4 Philippe Zinck^{2*}

5
6
7
8 ¹ Sustainable Materials Lab, Department of Chemical Engineering, KU Leuven, campus Kulak Kortrijk,
9 Etienne Sabbelaan 53, box 7659, B-8500 Kortrijk, Belgium

10 *wim.thielemans@kuleuven.be

11
12 ² Université de Lille, CNRS, Centrale Lille, Univ. Artois, UMR 8181 - UCCS - Unité de Catalyse et Chimie
13 du Solide, F-59000 Lille, France

14 *philippe.zinck@univ-lille.fr

15
16 ³Organic Synthesis and Mass Spectrometry Laboratory (S²MOs), University of Mons - UMONS, 23 Place
17 du Parc, 7000 Mons, Belgium

18
19
20
21
22
23
24
25

26

27 **Abstract**

28 Surface modification of cellulose nanocrystals (CNC) by organocatalysed grafting through ring-opening
29 polymerization (ROP) of trimethylene carbonate was investigated. Organocatalysts including an amidine
30 (DBU), a guanidine (TBD), an amino-pyridine (DMAP) and a phosphazene (BEMP) were successfully
31 assessed for this purpose, with performances in the order TBD > BEMP > DMAP, DBU. The grafting ratio
32 can be tuned by varying the experimental parameters, with the highest grafting of 74% by weight obtained
33 in smooth conditions, *i.e* at room temperature in tetrahydrofuran with a low amount of catalyst. This value
34 is much higher than that of typical ring opening polymerizations of cyclic esters initiated from the surface
35 of cellulose nanoparticles. Additionally, DSC analysis of the modified material revealed the presence of a
36 glass transition temperature, indicative of a sufficient graft length to display polymeric behaviour. This is,
37 to our knowledge, the first example of cellulose nanocrystals grafted with polycarbonate arms.

38

39 **Keywords:**

40 Cellulose nanocrystals, Organocatalysis, Polycarbonate, Nanocellulose, Ring-opening polymerization

41 Chemical compounds studied in this article:

42 Trimethylene Carbonate (PubChem CID: 123834); 1,5,7-Triazabicyclo[4.4.0]dec-5-ene (PubChem CID:
43 79873); 4-Dimethylaminopyridine (PubChem CID: 14284); BEMP phosphazene (PubChem CID:
44 3513851); 1,8-Diazabicyclo(5.4.0)undec-7-ene (PubChem CID: 81184)

45

46 **1. Introduction:**

47 Polysaccharides, and in particular cellulose, have experienced a rejuvenation of interest in recent years after
48 being slowly replaced by petroleum alternatives during the 20th century in many applications. With the
49 increasing concern over sustainability of many aspects of chemistry and materials science, the surge of
50 interest in these materials is unsurprising as they constitute the bigger fraction of biomass (Habibi, Lucia,
51 & Rojas, 2010). Cellulose nanoparticles in particular have received a lot of attention due to native cellulose
52 availability and their interesting properties such as a high aspect ratio, high young modulus, and low density
53 (Dufresne, 2013). Both cellulose nanofibrils (CNF) and cellulose nanocrystals (CNC) have been widely
54 studied as fillers for composite materials since the work of Favier *et al.* in 1995 who reported on the first

55 composites reinforced with cellulose nanocrystals. Incorporation of nanocellulose into a polymer matrix has
56 since been studied extensively and has the potential, especially when combined with biodegradable
57 polymers, to produce strong yet fully biodegradable materials. To this end, carbonates are of particular
58 interest, as aliphatic polycarbonates are highly valuable polymers with a very large scope of applications,
59 most notably in textiles, biomedical applications, microelectronics, and packaging (Yu, 2021). As an
60 additional benefit to being biodegradable (Artham & Doble, 2008), aliphatic polycarbonates have also been
61 obtained from renewable sources making them valuable as a potential alternative to petroleum-based
62 polymers (Helou *et al.*, 2010). To produce high performance composite materials, using nanocellulose
63 directly as an additive to polymers has proven to give less than ideal results due to the highly hydrophilic
64 nature of cellulose and its tendency to aggregate. These issues typically lead to a lower than expected
65 mechanical strength and ductility as these are highly dependent on the dispersion of the reinforcing fibre in
66 the polymer matrix and on the strength of the interface (Habibi, 2014).

67 To find solutions, a large amount of work has been carried out on the surface modification of cellulose
68 nanocrystals, typically using the hydroxyl groups (Eyley & Thielemans, 2014) *via* acetylation (Xu, Wu. Z.,
69 Wu. Q., Kuang, 2020), carbamation (Girouard *et al.*, 2016), esterification (Trinh & Mekonnen, 2018),
70 etherification (Sahlin *et al.*, 2018), silanization (Anžlovar, Krajnc, & Žagar, 2020), amidation (Lasseguette,
71 2008), and polymer grafting by different methods. While “grafting to” polymerization, *i.e* the process of
72 grafting a pre-synthesized polymer chain to the surface of cellulose can be successful (Azzam *et al.*, 2016),
73 the “grafting from” method is usually the preferred pathway to cellulose modification with polymers as it is
74 better controlled and avoids problems such as steric hindrance (Wohlhauser *et al.*, 2018). The “grafting
75 from” approach has been used to couple many types of polymers on cellulose such as *e.g* polylactones
76 (Habibi *et al.*, 2008; Labet & Thielemans, 2012) and polylactide (Lalanne-Tisné, Mees, Eyley, Zinck, &
77 Thielemans, 2020). In the case of polymer grafting, the main goal is usually to increase the compatibility
78 between the cellulose fibres and a polymer matrix (Thielemans, Belgacem, & Dufresne 2006). Lactones and
79 lactides have received a lot of attention due to their potential in biomedical application (Albertsson &
80 Varma, 2003) as they can undergo hydrolysis *in vivo*. However, polyester hydrolysis generates carboxylic
81 acids, which can be a significant drawback (Lendlein & Langer 2002). Polycarbonates demonstrate much
82 of the same advantages as polyesters when it comes to their degradation *in vivo* (Engler *et al.*, 2013) but
83 they do not generate acidic products during hydrolysis (Kluin *et al.*, 2009). Despite their potential use,
84 however, polycarbonate grafting has not seen much attention, with only some work on grafting on cellulose
85 filter paper (Pendergraph, Klein, Johansson, & Carlmark 2014), synthesis of isosorbide-based
86 polycarbonates (PC) in the presence of cellulose nanocrystals (Park *et al.*, 2019), and grafting of
87 poly(trimethylene carbonate) from starch (Samuel *et al.*, 2014). To our knowledge, the grafting of aliphatic
88 polycarbonates from the surface of cellulose nanocrystals has never been reported before.

89 To exert control over final properties, it is important to have a well-controlled polymerization reaction.
90 Therefore, the choice of a catalytic system with a high activity and a high level of control is a primary
91 concern. In the case of aliphatic polycarbonates, ring-opening polymerization (ROP) is currently the leading
92 approach as it leads to a living polymerization, therefore satisfying the criteria listed before, *i.e* high activity
93 and high level of control (Jerome & Lecomte, 2008; Penczek, Cypryk, Duda, Kubisa, & Slomkowski, 2007).
94 State of the art ROP allows for the use of many catalysts, including non-toxic metal centres like zinc.
95 However the presence of catalyst traces in the material produced is unwanted for many applications, and
96 metal catalysts are known for being hard to remove completely from polymeric materials (Hafrén &
97 Córdova, 2005). “Immortal” ring-opening polymerization is an approach that has been used for carbonate
98 polymerization and which allows for the use of a small amount of catalyst along with a co-initiator in the
99 form of a protic source. This co-initiator determines the number of chains growing, which gives control over
100 the chain length no matter the quantity of catalyst used while keeping a high catalytic activity (Helou,
101 Miserque, Brusson, Carpentier, & Guillaume, 2008). This approach can also be carried out metal free, as
102 many advances in organocatalysis have led to the emergence of a wide variety of ROP catalysts (Ottou,
103 Sardon, Mecerreyes, Vignolle, & Taton, 2016). While not all these systems are as efficient as metallic
104 catalysts, some are very promising and have shown a high degree of control. In the case of aliphatic
105 carbonates, and in particular trimethylene carbonate (TMC, see Figure 1), base catalysts have been reported
106 to produce polycarbonates with low dispersity (Kamber *et al.*, 2007). Catalysts of interest include amines
107 (dimethylethanolamine, 4-dimethylaminopyridine-DMAP), guanidines (1,5,7-triazabicyclo[4.4.0]dec-5-
108 ene-TBD), amidines (1,8-diazabicyclo[5.4.0]undec-7-ene-DBU), and phosphazenes (2-*tert*-butylimino-2-
109 diethylamino-1,3-dimethylperhydro-1,3,2-diazaphosphorine-BEMP) among others (Helou *et al.*, 2010;
110 Lohmeijer *et al.*, 2006). While ring-opening polymerization of trimethylene carbonate with organic catalysts
111 has been studied extensively in the last decade, small protic molecules such as benzyl alcohol were mostly
112 used as the co-initiator (Helou *et al.*, 2010). Therefore, using cellulose nanocrystals as the protic source to
113 obtain a brush copolymer with polycarbonate is an interesting perspective. Understanding of the reaction
114 and the influence of different parameters would be valuable to increase the general efficiency of polymer
115 grafting on cellulose, a process with a generally low yield (Lalanne-Tisné *et al.*, 2020). In particular, to our
116 knowledge, trimethylene carbonate has never been grafted on the surface of cellulose nanocrystals before.
117 Hence, we report the first synthesis of poly(trimethylene carbonate) grafted cellulose nanocrystals *via* ring
118 opening polymerization and investigate the influence of experimental parameters in an effort to increase the
119 grafting efficiency.

120

121

122 2. Materials and Methods

123 2.1. Materials

124 Sulfuric acid (97%) was obtained from VWR and calcium hydride was purchased from Acros Organics.
125 Dichloromethane and ethanol (analytical reagent grade) were obtained from Carlo Erba and cotton wool
126 was obtained from Fischer Scientific. Benzoic acid (99%) and tetrahydrofuran were obtained from Sigma
127 Aldrich and purified through alumina column (Mbraun SPS). 2-*tert*-Butylimino-2-diethylamino-1,3-
128 dimethylperhydro-1,3,2-diazaphosphorine (BEMP, 98%) was also obtained from Acros Organics. 1,8-
129 Diazabicyclo[5.4.0]undec-7-ene (DBU, 99%) was bought from Alpha Aesar and 1,5,7-
130 Triazabicyclo[4.4.0]dec-5-ene (TBD, >98%) from TCI. BEMP, DBU and TBD were introduced, opened
131 and stored in a glovebox and used as received.

132 Trimethylene carbonate (TMC, 99.5%) was purchased from Actuell Chemicals and purified by drying over
133 calcium hydride, filtered under inert atmosphere and then recrystallised. The purified monomer was
134 subsequently stored in a glovebox. 4-Dimethylaminopyridine (DMAP, 99%) was purchased from Aldrich
135 and co-evaporated three times with toluene followed by sublimation under vacuum at 85°C and stored in a
136 glovebox before use.

137 All chemicals were used as received unless stated otherwise.

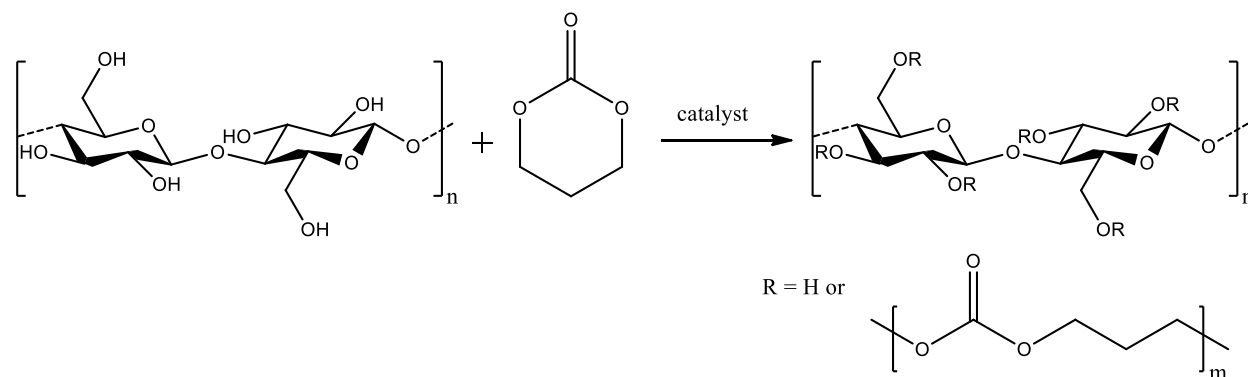
138 Preparation of CNCs

139 Cotton nanocrystals were prepared by acid hydrolysis of cotton wool for 35 min at 45°C in a 64 wt% aqueous
140 H₂SO₄ solution while stirring constantly (Revol *et al.*, 1992). Deionised water was used to wash the resulting
141 suspension by three successive centrifugations at 10 000 rpm and 10°C for 40 min, replacing the supernatant
142 with deionised water each time. Dialysis under continuous tap water flow was then used to remove residual
143 free acids. After 48 h, the pH of the eluent was checked to be neutral and a homogeneous dispersion of
144 cotton nanocrystals in water was obtained using a Branson sonicator at 10% amplitude for 2 min. The
145 dispersion was subsequently filtered over a fritted glass filter no. 2, and stirred overnight with Amberlite
146 MB-6113 resin to remove non-H₃O⁺ cations. The dispersion was sonicated one last time, frozen in liquid
147 nitrogen, and freeze-dried using a Heto PowerDry PL6000 apparatus from Thermo Scientific under a
148 vacuum of 2 bars. In addition to this procedure commonly followed in the literature to prepare cellulose
149 nanocrystals, a further purification was performed to remove surface adsorbed impurities that adsorb onto
150 the nanocrystal surface (Labet & Thielemans, 2011). After freeze-drying, the cotton nanocrystals were
151 Soxhlet extracted for 24h using ethanol as a solvent. The nanocrystals were subsequently dried in a vacuum
152 oven (0.5 bar) at 50°C and then dried further under ultra-high vacuum (Pfeiffer DCU 100) at 10⁻⁶ bars for 4

153 days. The container used for the drying process was then tightly closed, filled with argon, and placed in a
154 glovebox.

155 2.2. Ring-opening polymerization of TMC on CNC surface

156 All experiments were carried out under inert atmosphere in a glovebox unless stated otherwise.



158 *Figure 1: General reaction scheme of the ring-opening polymerization of trimethylene carbonate co-initiated by hydroxyls present*
159 *on the surface of cellulose nanocrystals*

160 In a typical reaction, a stir bar was placed in a small reactor, along with a specified amount of CNCs. The
161 molar ratio used are specified in Table 1 and Table 2 and based of the molecular weight of one glucose ring
162 bearing one primary OH. THF was added and the mixture was stirred for 30 minutes to disperse the CNCs.
163 Trimethylene carbonate was then added and left to stir until complete dissolution. Subsequently, the catalyst
164 was added while stirring and the reactor was placed in an oil bath set at a given temperature. After the
165 desired duration, the reaction was quenched using benzoic acid and dichloromethane addition, and the
166 mixture was filtered through a Soxhlet extraction thimble. A sample of the crude mixture was taken for
167 NMR analysis, and the modified CNCs were purified by Soxhlet extraction twice, first with
168 dichloromethane (24 hours), and then with ethanol (24 hours).

169 The modified nanocrystals were then dried under vacuum on a Schlenk line (< 1 mbar) for 24 hours.

170 The homopolymer produced as a side reaction was recovered from the first Soxhlet extraction mixture after
171 evaporation of the dichloromethane.

172 Characterization methods, apparatus, calculation method to determine grafting, conversion and yield, and
173 additional information about experimental procedures are all available in Supporting Information Appendix
174 A.

175 3. Results and discussion

176 3.1. Catalyst screening

Table 1: Ring-opening polymerization of TMC initiated from the surface of CNC in the presence of various organocatalysts at 25°C in THF

Entry	Catalyst	TMC / Catalyst / OH ^[a]	Time (h)	Polycarbonate grafting ^[b] (wt%)	Conversion ^[c] (%)	Grafting Yield ^[d] (%)	M _n homopolymer ^[e] (g.mol ⁻¹)	Đ _M ^[f]
1	Blank	500/0/50	5	2	4	0.3	NA	NA
2	TBD	500/1/50	5	51	99	16.5	19700	1.8
3	BEMP	500/1/50	3	24	45	5.0	35400	1.9
4	BEMP	500/1/50	5	35	52	8.6	33500	1.8
5	BEMP	500/1/50	16	37	52	9.3	33500	1.8
6	DMAP	500/0.5/50	5	13	6	2.4	NA	NA
7	DMAP	500/2/50	5	3	7	0.5	NA	NA
8	DMAP	500/5/50	5	12	6	2.2	2100	1.2
9	DBU	500/1/50	3	18	9	3.5	NA	NA
10	DBU	500/1/50	5	12	8	2.2	NA	NA

[a] Calculated using moles of glucose rings (162.14 g/mol), and considering 1 primary OH per ring [b] Determined by elemental analysis (calculation based on hydrogen content (%H) and carbon content (%C)) and corrected for adsorbed water using TGA. [c] Calculated *via* ¹H NMR to determine monomer/polymer ratio and corrected to include monomer grafted [d] Ratio of initial monomer to monomer grafted. [e] Determined by SEC of homopolymer vs. polystyrene standards and corrected with a correction factor of 0.57, 0.73 or 0.88 based on size measured (Palard *et al.* 2007). [f] Molar mass distribution calculated from SEC of homopolymer.

177 The performances of the different organic catalysts, namely TBD, BEMP, DMAP and DBU (shown in
 178 Figure 2) to polymerize TMC from the surface of cellulose nanocrystals were evaluated in THF at room
 179 temperature. The different catalysts were selected from their ability to catalyse ROP of TMC in the presence
 180 of an alcohol (Helou *et al.*, 2010). The TMC/catalyst/OH ratio was mostly kept at 500/1/50. Table 1 displays
 181 the most significant results.

182 In the absence of catalyst, significant conversion of the monomer into either grafts or homopolymer was not
 183 achieved (Table 1, entry 1), showing the clear need to use a catalyst.

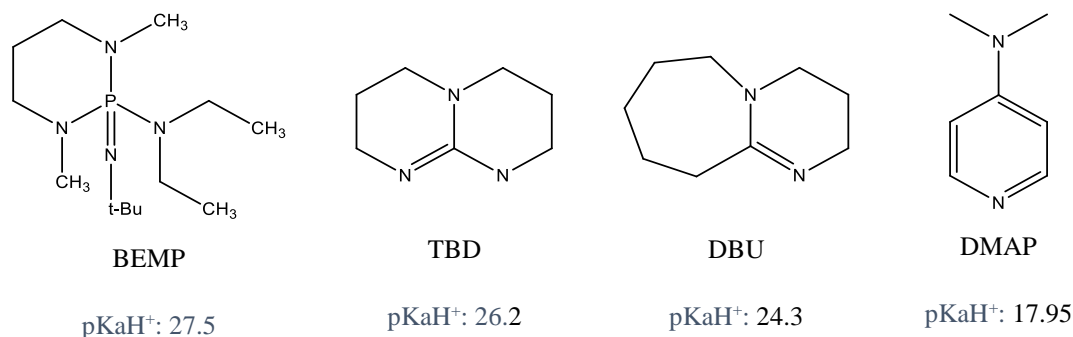


Figure 2: Structure of the organocatalysts used in this study. pKa values in acetonitrile (Ishikawa, 2009; Kaljurand *et al.*, 2005)

184 At a typical ratio of 500/1/50 (TMC/catalyst/OH), TBD was shown to reach full conversion of the monomer
185 within 5 hours, and resulted in modified CNCs containing of 51% grafted polymer (Table 1, entry 2), a
186 fairly high value for typical “grafting from” of polymer through ring opening polymerization from the
187 surface of nanocellulose. Similarly, a significant amount of monomer was converted to homopolymer (yield
188 of 16% for grafting), which shows an important competition between grafting of the monomer and
189 homopolymerization. However, it is common for grafting on cellulose to use a large excess of monomer to
190 increase the amount of grafting at the cost of efficiency (Lalanne-Tisné, *et al.*, 2020; Miao & Hamad, 2016).
191 Molar mass dispersity of the homopolymer was found at an acceptable value of 1.8 that is significantly
192 higher than usual values obtained for typical homopolymerizations (Nederberg *et al.*, 2007). The broader
193 distribution can be explained because it is a side reaction involving water and ethanol as co-initiators that
194 are still entrapped in the CNCs after purification. In addition, water and ethanol can also be involved in
195 hydrolysis and transcarbonatation reactions respectively. This can be seen from the MALDI ToF mass
196 spectra of the precipitated polymer showing the corresponding chain ends (details in Supporting Information
197 Appendix A).

198 Using similar reaction conditions for BEMP (entries 3-5), a phosphazene catalyst, showed quite different
199 results. Full conversion was not reached, and after increasing the reaction time from 3 to 5 hours, BEMP
200 conversion only reached 52%. Further increasing the reaction time to 16 hours did not increase monomer
201 conversion. Despite the lower conversion values, grafting on cellulose was achieved with this catalyst, and
202 up to 37% grafts were achieved in the modified CNCs, showing that this catalyst, while less efficient than
203 TBD using similar parameters, leads to substantial grafting.

204 The reactions conducted with DMAP (entries 6-8) and DBU (entries 9-10) did not perform as well as the
205 others under the same reaction conditions (room temperature, 5h), with NMR analysis showing very low
206 conversion. The resulting grafting was rather low for both catalyst (18% maximum) under these conditions,
207 and no oligomers could be recovered by precipitation to allow for SEC analysis. This is believed to be due
208 to their likely low average molecular weight.

209 We can try to explain the superior performance of TBD. TBD, unlike the other catalysts tested, possesses a
210 secondary amine group, giving it great potential for catalysis *via* hydrogen bonding. It is also interesting to
211 note that unlike DBU, which can operate by a basic and a nucleophilic mechanism, TBD can catalyse
212 transesterification reactions by dual activation *via* H-bonding (Simón & Goodman, 2007; Stanley *et al.*,
213 2019). Having a catalyst that can use both mechanisms may result in a better reaction due to the ability of
214 the catalyst to go in between intermolecular bonding (similarly to how a protic solvent gives a better
215 dispersion of CNCs). In addition, DBU and DMAP may favour homopolymerization due to their ability to

216 perform a nucleophilic attack on the monomer, which is not the case for the BEMP phosphazene, that leads
217 to an intermediary grafting ratio.

218 When looking at results for homopolymerization of trimethylene carbonate (Helou et al. 2010), it is worth
219 noting that TBD is also the most active catalyst in bulk, and full conversion is achieved much faster at lower
220 temperatures when compared to DMAP and DBU. As the work presented here is carried out in solvent but
221 at room temperature, it is possible that the activity of some of the catalysts (except for TBD) is reduced as
222 the activation requires more energy. However, further testing at higher temperature with all the catalyst was
223 not explored as we observed browning of the CNC at temperatures as low as 40°C in the presence of THF
224 and TBD (see next section).

225 Comparing the pKa of all 4 bases, TBD in acetonitrile does not come up as the strongest base (25.96), with
226 BEMP having a higher pKa (27.5), despite its superiority when it comes to grafting TMC on cellulose. TBD
227 is however a stronger base than DMAP and DBU, which could explain partially the better results obtained
228 when comparing these 3 bases. As for BEMP, it is a much bulkier catalyst, therefore steric hindrance may
229 be the cause for the lower activity when compared to TMC, in particular for the grafting onto CNC. This
230 can be exemplified as despite the subpar grafting efficiency on CNCs with BEMP, the extracted
231 homopolymer showed a higher M_n than the homopolymer recovered after full conversion with TBD.

232 As the screening of catalysts showed a more efficient grafting with TBD, this reaction was studied further,
233 in order to assess the influence of the reaction conditions.

234 **3.2. Influence of experimental parameters for the TBD catalysed grafting**

235 As the polymerization of TMC has also been performed in bulk (Helou et al., 2010), the grafting reaction
236 on the surface on CNCs was also carried in bulk as comparison (entry 11, Table 2). Despite
237 homopolymerization of TMC being very quick under bulk conditions, the reaction with cellulose did not go
238 to full conversion within an hour. However, the polycarbonate content of modified CNCs did reach 47%, a
239 value comparable to the content obtained by grafting in THF. The viscosity is a major issue in bulk reactions
240 as the melted monomer is not a good medium to disperse CNCs, resulting in poor homogeneity of the final
241 material and a greater difficulty to redisperse the modified cellulose in solvent, rendering its use more
242 complicated. The high viscosity is also likely a cause for the lower conversion, as the reaction slows down
243 considerably with homopolymer production. Lastly, the bulk reaction, as expected, shows a much higher
244 dispersity for the synthesized homopolymer, indicating some loss of control over the polymerization
245 reaction.

246 THF was used as the main solvent as it had shown to dissolve well TBD, TMC, poly(trimethylene
 247 carbonate), and to be a good solvent for CNC dispersion. Some other common solvents were assessed, but
 248 worse results were obtained (additional information in SI).

249 *Table 2: Ring-opening polymerization of TMC initiated from the surface of CNC in the presence of TBD in THF for 5 hours*

Entry	TMC / Catalyst / OH ^[a] T	Polycarbonate grafting ^[b]	Conversion ^[c]	Grafting Yield ^[d]	M _n homopolymer ^[e]	Đ _M ^[f]	
	(°C)	(wt%)	(%)	(%)	(g.mol ⁻¹)		
2	500/1/50	25	51	99	16.5	19700	1.8
11 ^[g]	500/1/50	65	47	33	14.1	11200	3.0
12 ^[h]	500/1/50	25	60	99	23.8	19600	1.9
13	500/1/50	0	54	99	18.7	16500	2.0
14	500/1/50	40	51	99	16.5	14100	2.3
15	500/1/50	60	52	99	17.2	9700	1.8
16 ^[i]	500/1/50	25	7	99	1.2	NA	NA
17	500/1/40	25	49	99	12.2	18700	1.7
18	500/1/30	25	49	99	9.2	23100	1.7
19 ^[j]	500/1/50	25	53	99	17.9	12100	2.0
20	500/2/50	25	9	99	1.6	26700	1.8
21	500/5/50	25	9	99	1.6	2200	1.3
22	500/0.5/50	25	74	99	45.2	7100	1.8
23	500/0.25/50	25	64	78	28.2	11400	1.6
24	250/0.5/50	25	57	99	42.1	11100	1.7
25	125/0.5/50	25	47	99	56.3	4600	1.8
26	62.5/0.5/50	25	23	99	37.9	NA	NA
27	250/1/50	25	50	99	31.8	13700	1.9
28	125/1/50	25	41	99	44.1	12900	1.8

[a] Calculated using moles of glucose rings (162.14 g/mol), and considering 1 primary OH per ring [b] Determined by elemental analysis (calculation based on hydrogen content (%H) and carbon content (%C)) and corrected for adsorbed water using TGA. [c] Calculated *via* ¹H NMR to determine monomer/polymer ratio and corrected to include monomer grafted [d] Ratio of initial monomer to monomer grafted. [e] Determined by SEC of homopolymer *vs.* polystyrene standards and corrected with a correction factor of 0.57, 0.73, or 0.88 based on size measured (Palard *et al.* 2007). [f] Molar mass distribution calculated from SEC of homopolymer. [g] Bulk reaction. [h] Reaction done over 24 hours instead of 5. [i] Reaction performed outside the glovebox. [j] Stirred for 24h and sonicated prior to reaction to maximize dispersion of CNC. NA: not available as oligomers, i.e too short to precipitate in cold methanol

250 As shown previously (entry 11), the polymerization of TMC was total after 5 hours, however a reaction in
 251 similar conditions was also performed over 24 hours (entry 12) to evaluate the activity of TBD over longer
 252 period of time, as it has been reported to be capable of depolymerization (Meimoun *et al.*, 2020). In the case
 253 of poly(trimethylene carbonate) grafted CNCs, a small increase in grafting content can be measured after
 254 24 hours of reaction, however the average molecular weight of the produced homopolymer started
 255 decreasing, showing potential signs of depolymerization or transcarbonation reactions. Therefore 5 hours
 256 was the favoured reaction time for most reaction, as it allowed for a good control over grafting while having
 257 good conversion, and a very good reproducibility (repeated reactions available in SI).

258 At the typical ratio of TMC/Cat/OH of 500/1/50, variation in temperature was tested to determine its
259 influence on the grafting reaction. At first glance, the temperature did not appear to change the amount of
260 grafting by a significant amount, as increasing the temperature to 40°C (entry 14) or 60°C (entry 15) yielded
261 CNCs with 51% and 52% grafts respectively (compared to entry 2). However, at temperatures as low as
262 40°C, browning of the CNCs was observed and became more pronounced at higher temperature, indicating
263 a potential degradation of the material. A shortening of the homopolymer chains is further observed as the
264 reaction temperature increases, indicating of possible depolymerization / chain scission reactions in the
265 presence of TBD, which has been reported for both polycarbonates (Li, Sablong, van Benthem, & Koning,
266 2017) and polylactides (Meimoun et al., 2020). A reaction at 0°C was also performed using an ice bath to
267 determine if a lower temperature could favour grafting over homopolymerization (entry 13), however the
268 results obtained for the grafting of CNC were in the same range (>50%) as the reaction performed at room
269 temperature (RT). The temperature used for the rest of the reaction was therefore set to RT (controlled by
270 an oil bath) to avoid any degradation of the material and to keep the reaction more energy efficient.

271 A reaction was then performed under inert atmosphere, but not under glovebox conditions, to evaluate how
272 sensitive the efficiency of the grafting was regarding the presence of water and other impurities (entry 16).
273 Prior to the reaction, CNCs and TMC were dried using a vacuum and an argon line rather than ultra-high
274 vacuum. THF was used after purification over alumina, similarly to experiments performed inside the
275 glovebox. Multiple argon/vacuum cycles were used to ensure inert atmosphere was achieved. Under these
276 conditions, a low amount of grafting (7 vs. 51% in entry 2) as well as the short chain length of the
277 homopolymer (impossible to precipitate in cold methanol) showed the prevalence of initiation by traces of
278 water and ethanol. Due to CNCs being hydrophilic, it is hard to remove significant traces of water from
279 them without extreme conditions (10^{-6} bar of vacuum), as well as ethanol from the purification steps of
280 preparing CNCs. This reaction shows that in order to maximize grafting efficiency purification of the
281 different chemicals a thorough drying of the cellulose is required, and working in a glovebox is useful.

282 In an attempt to increase grafting on cellulose, reactions were then performed with an increased ratio of
283 TMC/CNC by decreasing the quantity of cellulose used. Surprisingly, increasing the quantity of monomer
284 did not lead to a significant improvement in the grafting amount on cellulose (entries 17-18), which seems
285 to reach a maximum at around 50%, a result similar to other reactions (entry 2). This shows that simply
286 increasing the quantity of monomer used in the reaction is an ineffective way to increase the maximum
287 amount of grafting on the surface of CNC.

288 To determine if the availability of the hydroxyl groups on the surface of cellulose is an important factor, a
289 reaction was performed on a batch of CNC in THF with increased effort at individualization of CNCs. The
290 mixture of cellulose and solvent was prepared in the glovebox, then closed tightly and stirred over 24 hours

291 vs. 30 min previously used. A sonication bath was also used in burst of 5 minutes over the 24 hours. The
292 results obtained (entry 19) when compared to a “typical” reaction showed that increased effort for maximum
293 individualization of CNCs did not have a significant impact as the grafting obtained was also around the
294 50% mark.

295 The influence of catalyst loading was further assessed. Using a typical ratio TMC/TBD/OH of 500/1/50
296 showed good results and a grafting of around 50%. Increasing the catalyst ratio to 2 equivalents vs. OH
297 (entry 20) however lowered the grafting % on CNCs by a significant amount, whereas the length of the
298 homopolymer increased, indicating that increasing the TBD amount favours homopolymerization.
299 Increasing the amount of catalyst further to 5 equivalents (entry 21) yielded a similar amount of grafting
300 onto the CNCs than entry 20 (9%), but the average molecular weight of the isolated polymer was
301 significantly smaller ($< 3000 \text{ g.mol}^{-1}$). As mentioned previously, TBD is not only capable of polymerization,
302 but also depolymerization under the right circumstances *via* a nucleophilic attack on the carbonyl moieties
303 (Meimoun *et al.* 2020). In the case of polylactide, the use of 5 equivalents of TBD decreased the average
304 molecular of the resulting polymer more than tenfold, a result very similar to what is observed in this work
305 for the polycarbonate.

306 As opposed to increasing the catalyst quantity, lowering the amount of TBD used for the reaction to 0.5
307 equivalents showed an improvement in the grafting on CNCs with a material composed of up to 74%
308 polycarbonate grafts by weight and a grafting yield of 46% (entry 22). M_n of the homopolymer obtained
309 was lower, which can simply be explained by the increased quantity of monomer turned into grafts rather
310 than homopolymer.

311 Decreasing the quantity of catalyst further resulted in a decrease in the amount of grafting to 64% (entry
312 23), which is an improvement over the result obtained with 1 equivalent (entry 2) but a setback compared
313 to reactions performed with 0.5 equivalent (entry 22). Moreover, the low concentration of TBD led to a
314 slower reaction, and obtaining full conversion became more difficult.

315 To improve the grafting efficiency with respect to the total amount of monomer used, reactions with 0.5
316 equivalent of TBD (shown to have the best results) and successively lower amounts of monomer were
317 carried out.

318 The grafting % decreased from 74% to 57% (entry 22 vs. 24) when the monomer concentration was halved,
319 but the grafting yield stayed within the same range at 42%. While this is not an improvement, it however,
320 allows one to obtain CNCs with around 50% grafts with significantly less monomer loss than some previous
321 experiments (*e.g* entry 2). Lowering the amount of monomer further continued to reduce the % grafting

322 (47%) but led to an increased yield of 56% which is a good value for grafting of a polymer on cellulose, as
323 this parameter is usually overlooked in favour of trying to reach a maximum amount of grafting.

324 A similar reaction was also performed with a typical 1 equivalent TBD to compare to the grafting yield
325 obtained with 0.5 equivalents. As previously shown, the grafting % obtained is superior using a lower
326 quantity of catalyst, leading to a higher grafting yield.

327 Overall, this shows that a wide range of grafting % is possible, and specific values can be targeted using the
328 right amount of catalyst (typically 0.5 eq) without having to use a large excess of monomer, while keeping
329 the grafting yield as high as possible.

330 3.3. Characterization of the poly(trimethylene carbonate)-grafted CNC as a function of 331 the grafting ratio

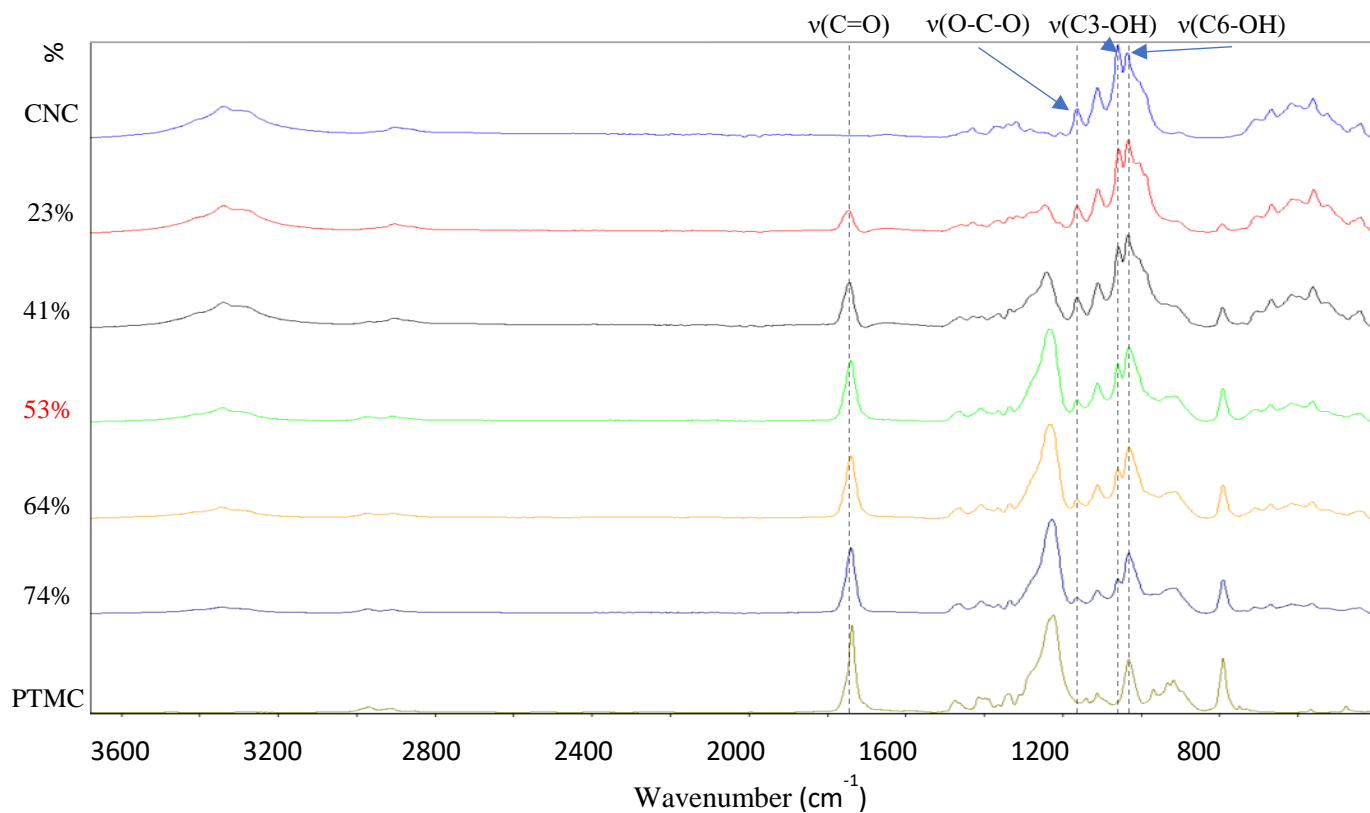


Figure 3: FT-IR spectra of unmodified cellulose nanocrystals (CNC) and grafted one with different graft content after purification by Soxhlet extraction. PTMC of 154000 g/mol extracted from soxhlet and purified by precipitation. Grafted CNCs corresponding to refer

332
333 In addition to elemental analysis, FT-IR was used to determine the success of the grafting reaction (Figure
334 3). As expected, both modified and unmodified cellulose spectra resemble each other. However, 2 bands
335 characteristic to our grafts are visible for modified cellulose. First, the band at 1754 cm⁻¹ can be identified

336 as a carbonyl stretch $\nu(\text{C}=\text{O})$, thus confirming the successful incorporation of the carbonate moieties onto
 337 CNCs. A second characteristic band is observed at 1229 cm^{-1} corresponding to $\nu(\text{C}-\text{O})$ stretching (Nyquist
 338 & Potts, 1961). As shown in Figure 3, the relative intensity of both bands increased with the grafting content,
 339 thus confirming the results determined by elemental analysis and TGA. Lastly, the ratio of absorption band
 340 at 1059 cm^{-1} corresponding to $\nu(\text{C3-OH})$ to C-O-C stretching at 1160 cm^{-1} (Marechal & Chanzy, 2000),
 341 decreases with increasing grafting ratio which shows the successful esterification of the secondary alcohol
 342 in the C3 position. The band at 1032 cm^{-1} corresponding to $\nu(\text{C6-OH})$ increases with increasing grafting
 343 ratio, as terminal OH of the polycarbonate chains appear in this region as well. As a consequence, grafting
 344 on the C6 position is not “visible” by FTIR, as both primary and secondary C-OH of cellulose are replaced
 345 by the primary terminal C-OH of the polymer at 1032 cm^{-1} . Note that $\nu(\text{C2-OH})$ cannot be discussed here
 346 as the polymer has a band in the area.

347 X-ray photoelectron spectroscopy can give additional insight into the composition of the modified CNCs at

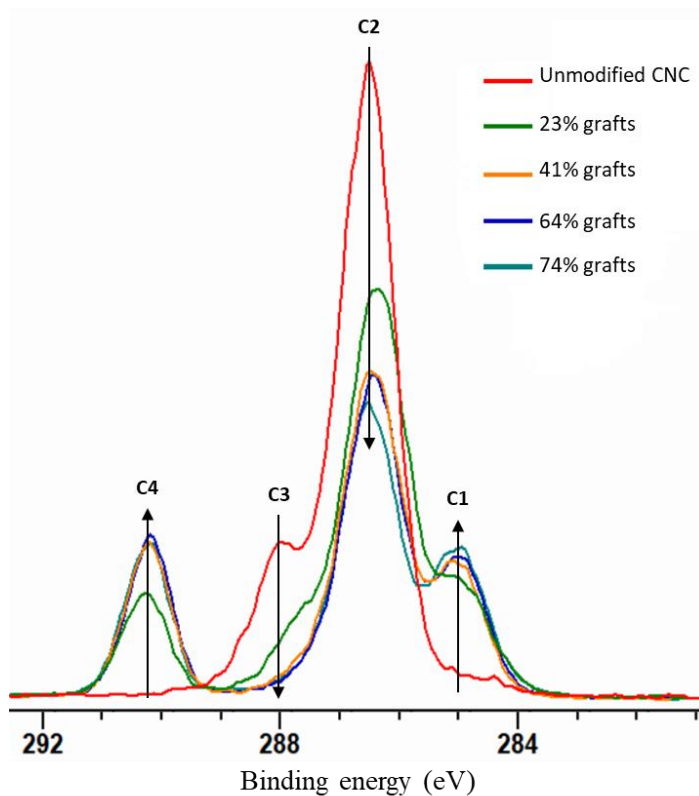


Figure 4: Carbon 1s X-ray photoelectron spectroscopy (XPS) scan of cellulose nanocrystals grafted with different poly(trimethylene carbonate content). Grafted CNCs corresponding to reference in Table 2: entry 26 (23%) entry 28 (41%), entry 23 (64%), entry 22 (74%)

348 a surface level. In the C1s high resolution scan (Figure 4), the aliphatic C-C carbon contribution (C1) at 285
 349 eV is shown to increase rapidly with grafting, as cellulose units do not contain aliphatic carbons, unlike
 350 trimethylene carbonate. With an increasing amount of graft content, the relative intensity of the C1

351 contribution increases and then appears to reach a maximum, at the contribution amount expected for pure
352 poly(trimethylene carbonate) chains indicating that no cellulose contribution is visible anymore. As opposed
353 to C1, the C2 and C3 contributions to the C1s signal, corresponding to C-O and O-C-O environments
354 respectively, both decreased with an increasing amount of grafts, as poly(trimethylene carbonate)
355 contributes less to the C-O signal than cellulose, and does not contribute to the O-C-O signal. Finally, the
356 O-C=O contribution (C4) increased with grafting content, similarly to C1 as the carbonate function is the
357 only contribution to this peak. The results obtained from elemental analysis, along with form of
358 characterization are therefore confirmed with the XPS data.

359 With poly(trimethylene carbonate) being a highly hydrophobic material, grafting CNCs with it will change
360 its interaction with water significantly. To quantify this, grafted CNCs were used in contact angle

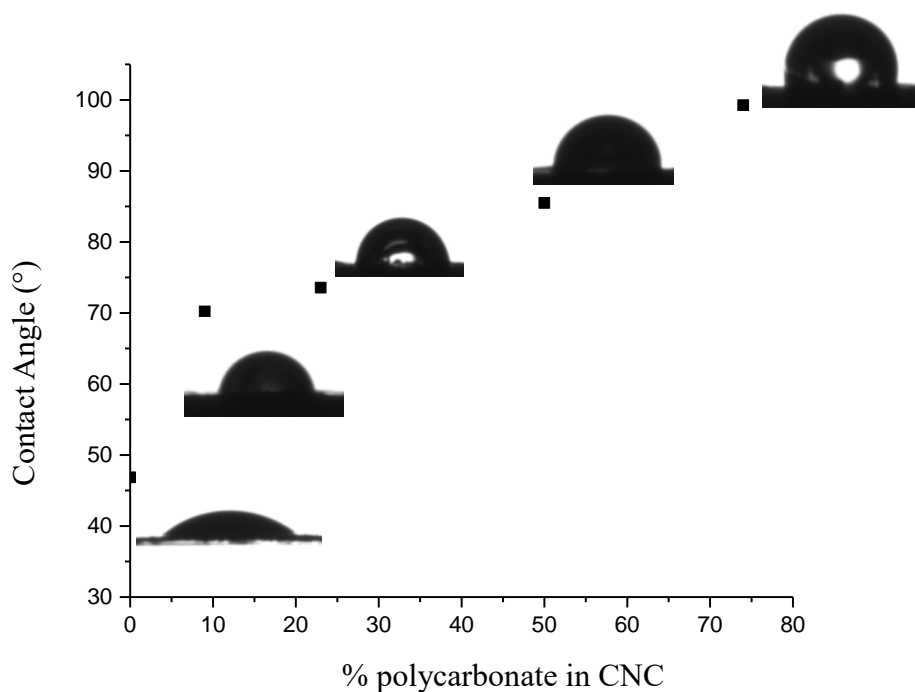


Figure 5: Contact angle of a water droplet on the surface of CNC modified with different polycarbonate content. Grafted CNCs corresponding to reference in Table 2: entry 9 (9%) entry 26 (23%), entry 2 (51%), and entry 22 (74%)

361 measurements with water. The water contact angle increased rapidly with the poly(trimethylene carbonate)
362 content of the cellulose sample (Figure 5), in line with the length of the graft in the brush copolymer
363 structure. For a poly(trimethylene carbonate) content as low as 9%, the increase in hydrophobicity is
364 significant, which then increases more slowly as the carbonate content increased, up to a value close to that
365 of pure PTMC reported in the range 90-110°C (Brossier et al., 2021; Yao et al., 2017). This might be related
366 to an increasing coverage of the CNC by PTMC, ranging from partial to almost full. It is noteworthy that
367 the contact angle and thus the wettability can be controlled by targeting the proper polycarbonate grafting

368 ratio. As a result, we believe that this increase in hydrophobicity shows good signs for the potential
369 incorporation of these nanoparticles in a polymer matrix for composite applications.

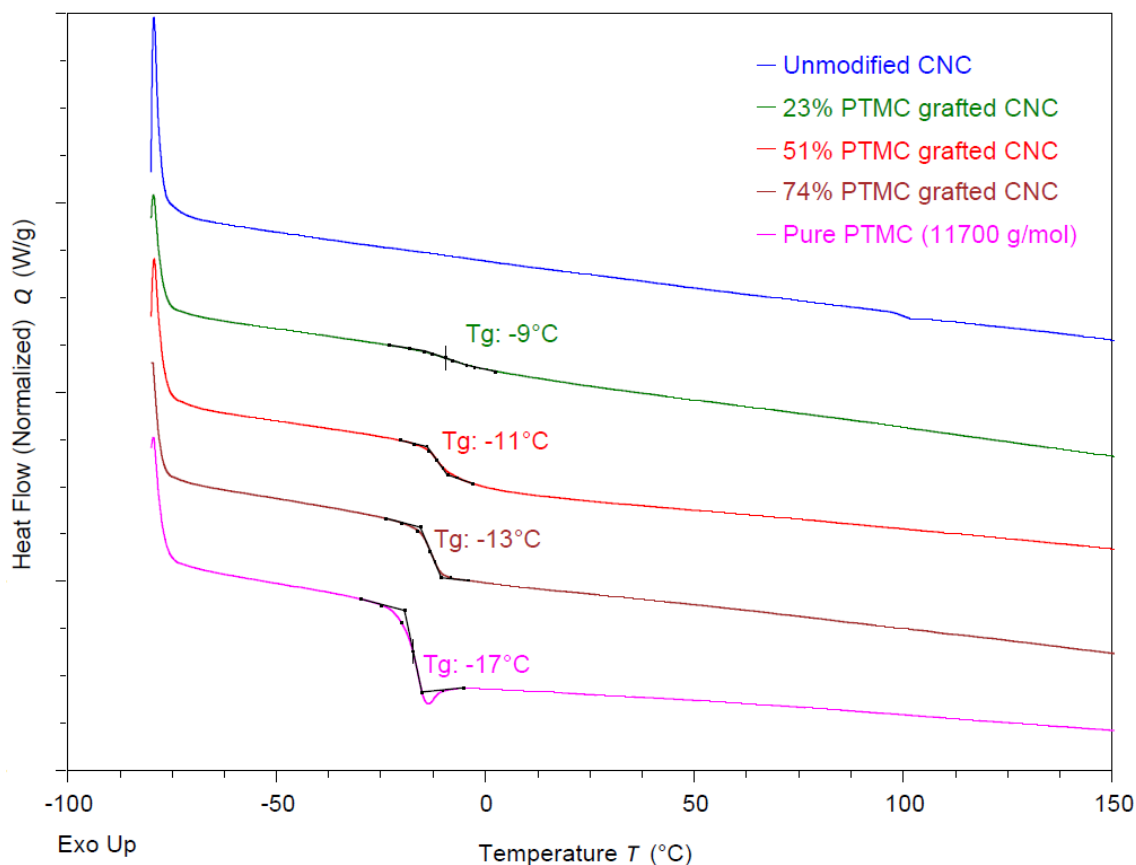


Figure 6: Differential Scanning Calorimetry graphs of CNC, poly(trimethylene carbonate) (PTMC) and modified CNC during the second heating at 10°C/min. . Grafted CNCs corresponding to reference in Table 2: entry 26 (23%), entry 2 (51%), and entry 22 (74%)

370 DSC analyses were conducted to obtain more information on the thermal behaviour of the grafts. The
371 samples were heated from -80 to 190°C, as the glass transition temperature (T_g) of poly(trimethylene
372 carbonate) is below 0 °C. For unmodified CNCs, no T_g or melting point were observed, as expected (Figure
373 6Figure 6). For grafted CNCs, a glass transition was observed for all samples in the same range as the T_g of
374 pure poly(trimethylene carbonate), but with slightly higher values. With a graft content as low as 23%, a T_g
375 at -9°C can be recorded, indicative of the presence of poly(trimethylene carbonate) grafts. As the carbonate
376 content increased, the T_g decreased and progressively moved towards the value for poly(trimethylene
377 carbonate) homopolymer (11700 g.mol⁻¹) at -17°C, without ever reaching it. This phenomenon could be
378 attributed to a lower mobility of the chain closer to the CNC backbone, their relative amount decreasing
379 with higher grafting values. Overall, this shows that polymer grafts on cellulose nanocrystals are of
380 sufficient length to showcase polymeric behaviour. In addition, we also measured the T_g of non-grafted
381 homopolymers of similar molecular weight and compared it with that of the grafted polymer (see SI section

382 S12). The 3 homopolymers of *ca.* 20 000 g/mol show a T_g of *ca.* -16/-17 °C, whereas the T_g of the grafted
383 CNC are in the range -10 to -13°C, which tend to confirm the occurrence of a true grafting.

384 In order to know whether the cellulose nanocrystals retain their structure following grafting, wide-angle X-
385 ray scattering was used to determine the crystallinity of the pristine and PTMC grafted CNC samples. The
386 X-ray scattering data was fitted with the crystal structure of cellulose I β , and the amorphous contribution to
387 the scattering determined. As no melting peak was seen in the DSC data, we know that the PTMC will be
388 included in the amorphous contribution to the scattering data. Therefore, considering the amount of PTMC
389 in the sample, changes in crystallinity of the cellulose ($\Delta\chi_{c, \text{cellulose}}$) can be determined as the difference in
390 crystallinity between the starting material and the product ($\Delta\chi_{c, \text{sample}}$), minus the expected contribution from
391 PTMC (ϕ_{PTMC} – the volume fraction of PTMC) as shown in Table 3.

392 *Table 3: The calculated sample crystallinity based on WAXS measurements for all samples*

Sample	$\chi_{c, \text{sample}}$	$\Delta\chi_{c, \text{sample}}$	ϕ_{PTMC}	$\Delta\chi_{c, \text{cellulose}}$
Unmodified CNC	0.99	-	0	0
23% PTMC-g-CNC	0.68	-0.31	0.27	-0.04
41% PTMC-g-CNC	0.56	-0.43	0.46	0.03
51% PTMC-g-CNC	0.37	-0.62	0.56	-0.06
64% PTMC-g-CNC	0.26	-0.73	0.69	-0.04
74% PTMC-g-CNC	0.14	-0.85	0.78	-0.07

393 The data on the grafted samples shows only around 5% change in cellulose crystallinity when the
394 contribution from amorphous PTMC is removed. This change could be due to peeling of the surface chains
395 of the CNC during grafting, however, given the lack of trend in $\Delta\chi_{c, \text{cellulose}}$, and the wide standard deviation
396 in the values, it is possible that this reflects the error in the calculation of the sample crystallinity by this
397 methodology.

398

399 Conclusion

400 Ring-opening polymerization (ROP) of trimethylene carbonate was performed using cellulose nanocrystals
401 as a co-initiator in the presence of 4 organocatalysts, *i.e.* DMAP, DBU, TBD and BEMP). The overall
402 performances considering conversion, grafting ratio and yield are TBD > BEMP > DBU, DMAP. After
403 optimization, a grafting ratio as high as 74% could be reached using TBD, corresponding to a material
404 composed by weight of almost $\frac{3}{4}$ polycarbonate grafts. The reaction was performed at room temperature
405 with a low concentration of the catalyst, 0.5% vs. TMC and 500 equiv. TMC per glucose unit. This led to a

406 material with T_g and contact angle close to that of poly(trimethylene carbonate). The use of a single step
407 reaction, under mild conditions while keeping grafting yield high is of great interest to produce CNC with
408 a controlled amount of grafts. Furthermore, we were able to show some of the most influential parameters
409 with respect to grafting content, providing some insight on the chemistry behind cellulose modification. The
410 contact angle can be tuned from *ca.* 50 to 100° by adjusting the grafting ratio. Lastly, DSC results revealed
411 the polymeric behaviour of the grafts, confirming the successful grafting of polycarbonate chains of
412 sufficient length to have high potential as reinforcement fillers in composite materials. To our knowledge,
413 this is the first reported chemical modification of cellulose nanocrystals with trimethylene carbonate, and
414 the first example of a ROP-based grafting from process attaching polycarbonate chains onto CNCs.

415

416 **4. Acknowledgement**

417 The authors are grateful to Aurélie Malfait for SEC measurements, and Gertrude Kignelman for the help
418 with contact angle analysis. The authors also acknowledge financial support from the Initiatives for
419 Science, Innovation, Territories and Economy (I-SITE) Lille Nord – Europe (MLT PhD fellowship), from
420 Research Foundation Flanders (grant G0C6013N), KU Leuven (grant C14/18/061) and from the European
421 Union’s European Fund for Regional Development, Flanders Innovation & Entrepreneurship, and the
422 Province of West-Flanders for financial support in the Accelerate³ project (Interreg Vlaanderen-Nederland
423 program). Université de Lille, Chevreul Institute (FR 2638), Ministère de l’Enseignement Supérieur de la
424 Recherche et de l’Innovation, Région Hauts de France are also acknowledged for supporting and funding
425 partially this work.

426

427 **5. References:**

- 428
429
430 Albertsson, A.-C., & Varma, I. K. (2003). Recent Developments in Ring Opening Polymerization of
431 Lactones for Biomedical Applications. *Biomacromolecules*, 4(6), 1466–1486.
- 432 Anžlovar, A., Krajnc, A., & Žagar, E. (2020). Silane modified cellulose nanocrystals and nanocomposites
433 with LLDPE prepared by melt processing. *Cellulose*, 27(10), 5785–5800.
- 434 Artham, T., & Doble, M. (2008). Biodegradation of Aliphatic and Aromatic Polycarbonates:
435 Biodegradation of Aliphatic and Aromatic Polycarbonates. *Macromolecular Bioscience*, 8(1), 14–24.
- 436 Azzam, F., Heux, L., & Jean, B. (2016). Adjustment of the Chiral Nematic Phase Properties of Cellulose
437 Nanocrystals by Polymer Grafting. *Langmuir*, 32(17), 4305–4312.
- 438 Brossier, T., Volpi, G., Vasquez-Villegas, J., Petitjean, N., Guillaume, O., Lapinte, V., & Blanquer, S.
439 (2021). Photoprintable Gelatin- *graft* -Poly(trimethylene carbonate) by Stereolithography for Tissue
440 Engineering Applications. *Biomacromolecules*, 22(9), 3873–3883.
- 441 Dufresne, A. (2013). Nanocellulose: a new ageless bionanomaterial. *Materials Today*, 16(6), 220–227.
- 442 Engler, A. C., Chan, J. M. W., Fukushima, K., Coady, D. J., Yang, Y. Y., & Hedrick, J. L. (2013).
443 Polycarbonate-Based Brush Polymers with Detachable Disulfide-Linked Side Chains. *ACS Macro Letters*,
444 2(4), 332–336.
- 445 Eyley, S., & Thielemans, W. (2014). Surface modification of cellulose nanocrystals. *Nanoscale*, 6(14),
446 7764–7779.
- 447 Favier, V., Chanzy, H., & Cavaille, J. Y. (1995). Polymer Nanocomposites Reinforced by Cellulose
448 Whiskers. *Macromolecules*, 28(18), 6365–6367.
- 449 Girouard, N. M., Xu, S., Schueneman, G. T., Shofner, M. L., & Meredith, J. C. (2016). Site-Selective
450 Modification of Cellulose Nanocrystals with Isophorone Diisocyanate and Formation of Polyurethane-CNC
451 Composites. *ACS Applied Materials & Interfaces*, 8(2), 1458–1467.
- 452 Habibi, Y. (2014). Key advances in the chemical modification of nanocelluloses. *Chem. Soc. Rev.*, 43(5),
453 1519–1542.

454 Habibi, Y., Goffin, A.-L., Schiltz, N., Duquesne, E., Dubois, P., & Dufresne, A. (2008). Bionanocomposites
455 based on poly(ϵ -caprolactone)-grafted cellulose nanocrystals by ring-opening polymerization. *Journal of*
456 *Materials Chemistry*, 18(41), 5002.

457 Habibi, Y., Lucia, L. A., & Rojas, O. J. (2010). Cellulose Nanocrystals: Chemistry, Self-Assembly, and
458 Applications. *Chemical Reviews*, 110(6), 3479–3500.

459 Hafrén, J., & Córdova, A. (2005). Direct Organocatalytic Polymerization from Cellulose Fibers: Direct
460 Organocatalytic Polymerization from Cellulose Fibers. *Macromolecular Rapid Communications*, 26(2), 82–
461 86.

462 Helou, M., Miserque, O., Brusson, J.-M., Carpentier, J.-F., & Guillaume, S. M. (2010). Organocatalysts for
463 the Controlled “Immortal” Ring-Opening Polymerization of Six-Membered-Ring Cyclic Carbonates: A
464 Metal-Free, Green Process. *Chemistry - A European Journal*, 16(46), 13805–13813.

465 Helou, M., Miserque, O., Brusson, J.-M., Carpentier, J.-F., & Guillaume, S. M. (2008). Ultraproductive,
466 Zinc-Mediated, Immortal Ring-Opening Polymerization of Trimethylene Carbonate. *Chemistry - A*
467 *European Journal*, 14(29), 8772–8775.

468 Ishikawa T, editor. Superbases for organic synthesis: guanidines, amidines and phosphazenes and related
469 organocatalysts. Chichester: John Wiley & Sons, Ltd; 2009; 336 pp

470 Jerome, C., & Lecomte, P. (2008). Recent advances in the synthesis of aliphatic polyesters by ring-opening
471 polymerization. *Advanced Drug Delivery Reviews*, 60(9), 1056–1076.

472 Kaljurand, I., Kütt, A., Sooväli, L., Rodima, T., Mäemets, V., Leito, I., & Koppel, I. A. (2005). Extension
473 of the Self-Consistent Spectrophotometric Basicity Scale in Acetonitrile to a Full Span of 28 p K a Units:
474 Unification of Different Basicity Scales. *The Journal of Organic Chemistry*, 70(3), 1019–1028.

475 Kamber, N. E., Jeong, W., Waymouth, R. M., Pratt, R. C., Lohmeijer, B. G. G., & Hedrick, J. L. (2007).
476 Organocatalytic Ring-Opening Polymerization. *Chemical Reviews*, 107(12), 5813–5840.

477 Kluin, O. S., van der Mei, H. C., Busscher, H. J., & Neut, D. (2009). A surface-eroding antibiotic delivery
478 system based on poly-(trimethylene carbonate). *Biomaterials*, 30(27), 4738–4742.

479 Labet, M., & Thielemans, W. (2011). Improving the reproducibility of chemical reactions on the surface
480 of cellulose nanocrystals: ROP of ϵ -caprolactone as a case study. *Cellulose*, 18(3), 607–617.

481 Labet, M., & Thielemans, W. (2012). Citric acid as a benign alternative to metal catalysts for the production
482 of cellulose-grafted-polycaprolactone copolymers. *Polymer Chemistry*, 3(3), 679

483 Lalanne-Tisné, M., Mees, M. A., Eyley, S., Zinck, P., & Thielemans, W. (2020). Organocatalyzed ring
484 opening polymerization of lactide from the surface of cellulose nanofibrils. *Carbohydrate Polymers*, 250,
485 116974.

486 Lasseguette, E. (2008). Grafting onto microfibrils of native cellulose. *Cellulose*, 15(4), 571–580.

487 Lendlein, A., Langer R. (2002). Biodegradable, Elastic Shape-Memory Polymers for Potential Biomedical
488 Applications. *Science*, 296(5573), 1673–1676.

489 Li, C., Sablong, R. J., van Benthem, R. A. T. M., & Koning, C. E. (2017). Unique Base-Initiated
490 Depolymerization of Limonene-Derived Polycarbonates. *ACS Macro Letters*, 6(7), 684–688.

491 Lohmeijer, B. G. G., Pratt, R. C., Leibfarth, F., Logan, J. W., Long, D. A., Dove, A. P., Nederberg, F., Choi,
492 J., Wade, C., Waymouth, R. M., & Hedrick, J. L. (2006). Guanidine and Amidine Organocatalysts for Ring-
493 Opening Polymerization of Cyclic Esters. *Macromolecules*, 39(25), 8574–8583.

494 Marechal, Y., & Chanzy, H. (2000). The hydrogen bond network in Ib cellulose as observed by infrared
495 spectrometry. *Journal of Molecular Structure*, 14.

496 Meimoun, J., Favrelle-Huret, A., Bria, M., Merle, N., Stoclet, G., De Winter, J., Mincheva, R., Raquez, J.-
497 M., & Zinck, P. (2020). Epimerization and chain scission of polylactides in the presence of an organic base,
498 TBD. *Polymer Degradation and Stability*, 181, 109188.

499 Miao, C., & Hamad, W. Y. (2016). In-situ polymerized cellulose nanocrystals (CNC)—poly(l -lactide)
500 (PLLA) nanomaterials and applications in nanocomposite processing. *Carbohydrate Polymers*, 153, 549–
501 558.

502 Nederberg, F., Lohmeijer, B. G. G., Leibfarth, F., Pratt, R. C., Choi, J., Dove, A. P., Waymouth, R. M., &
503 Hedrick, J. L. (2007). Organocatalytic Ring Opening Polymerization of Trimethylene Carbonate.
504 *Biomacromolecules*, 8(1), 153–160.

505 Nyquist, R. A., & Potts, W. J. (1961). Infrared absorptions of organic carbonate derivatives and related
506 compounds. *Spectrochimie Acts*, 17, 679-697.

507 Ottou, W. N., Sardon, H., Mecerreyes, D., Vignolle, J., & Taton, D. (2016). Update and challenges in
508 organo-mediated polymerization reactions. *Progress in Polymer Science*, 56, 64–115.

509 Ottou, W. N., Sardon, H., Mecerreyes, D., Vignolle, J., & Taton, D. (2016). Update and challenges in
510 organo-mediated polymerization reactions. *Progress in Polymer Science*, 56, 64–115.

511 Palard, I., Schappacher, M., Belloncle, B., Soum, A., & Guillaume, S. M. (2007). Unprecedented
512 Polymerization of Trimethylene Carbonate Initiated by a Samarium Borohydride Complex: Mechanistic
513 Insights and Copolymerization with ϵ -Caprolactone. *Chemistry - A European Journal*, 13(5), 1511–1521.

514 Park, S.-A., Eom, Y., Jeon, H., Koo, J. M., Lee, E. S., Jegal, J., Hwang, S. Y., Oh, D. X., & Park, J. (2019).
515 Preparation of synergistically reinforced transparent bio-polycarbonate nanocomposites with highly
516 dispersed cellulose nanocrystals. *Green Chemistry*, 21(19), 5212–5221.

517 Penczek, S., Cypryk, M., Duda, A., Kubisa, P., & Slomkowski, S. (2007). Living ring-opening
518 polymerizations of heterocyclic monomers. *Progress in Polymer Science*, 32(2), 247–28

519 Pendergraph, S. A., Klein, G., Johansson, M. K. G., & Carlmark, A. (2014). Mild and rapid surface initiated
520 ring-opening polymerisation of trimethylene carbonate from cellulose. *RSC Advances*, 4(40), 20737.

521 Revol, J.-F., Bradford, H., Giasson, J., Marchessault, R. H., & Gray, D. G. (1992). Helicoidal self-ordering
522 of cellulose microfibrils in aqueous suspension. *International Journal of Biological Macromolecules*, 14(3),
523 170–172.

524 Sahlin, K., Forsgren, L., Moberg, T., Bernin, D., Rigdahl, M., & Westman, G. (2018). Surface treatment of
525 cellulose nanocrystals (CNC): effects on dispersion rheology. *Cellulose*, 25(1), 331–345.

526 Samuel, C., Chalamet, Y., Boisson, F., Majesté, J.-C., Becquart, F., & Fleury, E. (2014). Highly efficient
527 metal-free organic catalysts to design new Environmentally-friendly starch-based blends. *Journal of*
528 *Polymer Science Part A: Polymer Chemistry*, 52(4), 493–503.

529 Simón, L., & Goodman, J. M. (2007). The Mechanism of TBD-Catalyzed Ring-Opening Polymerization of
530 Cyclic Esters. *The Journal of Organic Chemistry*, 72(25), 9656–9662.

531 Stanley, N., Chenal, T., Jacquél, N., Saint-Loup, R., Prates Ramalho, J. P., & Zinck, P. (2019).
532 Organocatalysts for the Synthesis of Poly(ethylene terephthalate- *co* -isosorbide terephthalate): A Combined
533 Experimental and DFT Study. *Macromolecular Materials and Engineering*, 304(9), 1900298.

534 Thielemans, W., Belgacem, M. N., & Dufresne, A. (2006). Starch Nanocrystals with Large Chain Surface
535 Modifications. *Langmuir*, 22(10), 4804–4810.

536 Trinh, B. M., & Mekonnen, T. (2018). Hydrophobic esterification of cellulose nanocrystals for epoxy
537 reinforcement. *Polymer*, 155, 64–74.

538 Wohlhauser, S., Delepierre, G., Labet, M., Morandi, G., Thielemans, W., Weder, C., & Zoppe, J. O. (2018).
539 Grafting Polymers *from* Cellulose Nanocrystals: Synthesis, Properties, and Applications. *Macromolecules*,
540 *51*(16), 6157–6189.

541 Xu, J., Wu, Z., Wu, Q., & Kuang, Y. (2020). Acetylated cellulose nanocrystals with high-crystallinity
542 obtained by one-step reaction from the traditional acetylation of cellulose. *Carbohydrate Polymers*, *229*,
543 115553.

544 Yao, H., Li, J., Li, N., Wang, K., Li, X., & Wang, J. (2017). Surface Modification of Cardiovascular Stent
545 Material 316L SS with Estradiol-Loaded Poly (trimethylene carbonate) Film for Better Biocompatibility.
546 *Polymers*, *9*(11), 598.

547 Yu, W., E. Maynard, Chiaradia, V., Arno, M.C., Dove, A.P. (2021) Aliphatic Polycarbonates from Cyclic
548 Carbonate Monomers and Their Application as Biomaterials, *Chemical Reviews*, *121*, 10865–10907.

549

550

551